Laser and Particle Beams (2006), *24*, 15–25. Printed in the USA.

DOI: 10.1017/S0263034606060046

Analytical description of rippling effect and ion acceleration in plasma produced by a short laser pulse

S. GLOWACZ,[1,2] H. HORA,[3] J. BADZIAK,[1] S. JABLONSKI,[1,2] YU CANG,[2,4] AND F. OSMAN[2]

[1]Institute of Plasma Physics and Laser Microfusion, Warsaw, Poland
[2]School of Quantitative Methods and Mathematical Sciences, University of Western Sydney, Penrith, Australia
[3]Department of Theoretical Physics, University of New South Wales, Sydney, Australia
[4]Institute of Physics, Chinese Academy of Sciences, Beijing, China

(RECEIVED 6 February 2005; ACCEPTED 7 April 2005)

Abstract

In this paper we present the analytical description of two processes dealing with the skin-layer ponderomotive acceleration method of fast ion generation by a short laser pulse: ion density rippling in the underdense plasma region and generation of ion beams by trapped electromagnetic field in plasma. Some numerical examples of hydrodynamic simulation illustrating these processes are shown. The effect of using the laser pulse consisting of different frequency components on the ion density rippling and on phenomena connected with trapped electromagnetic field is analyzed.

Keywords: Acceleration of plasma blocks; Density rippling; Laser beam smoothing; Laser-plasma interaction; Nonlinear (ponderomotive) force; Suppression of density rippling

1. INTRODUCTION

The skin-layer ponderomotive acceleration (S-LPA) mechanism (Hora *et al*., 2002; Badziak *et al*., 2004*a*, 2004*b*) is proposed to explain the observed features of ion beams produced at the interaction of a subrelativistic intensity ($\leq 10^{18}$ W/cm^2), high-contrast, ultrashort ($\leq$ 1 ps) laser pulse with a solid target. S-LPA assumes that electrons in the thin preplasma layer created in front of the target are accelerated by the ponderomotive force near the critical density surface where a mirror reflection takes place. Since ions are too heavy to be accelerated in the same way, the longitudinal electric field between electrons and ions plays a crucial role and has to be considered to explain motion of ions. S-LPA requires electrons to be closely attached to ions (the Debye length is much less than the thickness of accelerated plasma block). For subrelativistic laser intensities, this assumption is well justified. Experiments performed with sub-joule (1 ps) laser pulses interacting with different targets at intensities up to 2×10^{17} W/cm^2, showed that in the backward and forward direction, high density ion beams (plasma blocks) are generated (Badziak *et al*., 2004*a*, 2005). The ion current densities measured in these experiments reached high value, about 10^{10} A/cm^2. In experiments by Cang *et al.* (2005) and Glowacz *et al.* (2004), numerical calculations were presented which showed that parameters of ion beams observed in the experiments can be explained by the S-LPA mechanism. The density rippling process was recognized from numerical studies in 1974 at the University of Rochester (Hora, 1991, Figs. 10.10 and 10.11; Hoffmann *et al*., 1990; Asthana *et al*., 2000; Purohit *et al*., 2003; Saini & Gill, 2004), as the result of partial standing waves where the nonlinear (ponderomotive) forces pushes plasma faster to the nodes and than the other plasma dynamics would straighten the motion. The theory (Hora & Aydin, 1992) confirmed this mechanism and how this could be overcome by laser beam smoothing, especially by broad band irradiation (Hora & Aydin, 1992, 1999; Boreham *et al*., 1997; Osman *et al*., 2004). The following approach is specifically directed to analyze new developments in the plasma block generation (Hora *et al*., 2002; Badziak *et al*., 2004*a*, 2004*b*), as an alternative scheme for laser fusion (Hora, 2004; Osman *et al*., 2004), to be considered as one option of fast ignition (Bauer, 2003; Deutsch, 2004; Mulser & Bauer, 2004; Mulser & Schneider, 2004; Osman *et al*., 2004; Ramirez *et al*., 2004; Hoffmann *et al*., 2005; Badziak *et al*., 2005).

The interaction of laser light with preplasma in the underdense region causes density rippling which prevents laser energy from being transported and deposited near the criti-

Address correspondence and reprint requests to: Heinrich Hora, Department of Theoretical Physics, University of New South Wales, Sydney, Australia. E-mail: h.hora@unsw.edu.au

cal density. This results in the deterioration of the parameters of ion beams which are generated near the critical density surface. Methods of smoothing density rippling were described by Hora and Aydin (1992, 1999) and Boreham *et al*. (1997). In this paper, we present an analytical description of processes dealing with broad band picosecond laser smoothing. This smoothing method on ion beams generation will also be shown.

2. LONGITUDINAL ELECTRIC FIELD PRODUCED BY THE ELECTROMAGNETIC STANDING WAVE IN PLASMA

To find the longitudinal electric field between electron and ion fluids the Maxwell equations:

$$\frac{\partial^2}{\partial x^2} E_z(x,t) = \frac{1}{c^2}\frac{\partial^2}{\partial t^2} E_z(x,t) + \frac{1}{\varepsilon_0 c^2}\frac{\partial}{\partial t} j_z(x,t) \tag{1}$$

$$\frac{\partial}{\partial t} B_y(x,t) = \frac{\partial}{\partial x} E_z(x,y) \tag{2}$$

$$0 = \frac{1}{c^2}\frac{\partial^2}{\partial^2 t} E_x(x,t) + \frac{1}{\varepsilon_0 c^2}\frac{\partial}{\partial t} j_x(x,t) \tag{3}$$

and the Ohm's law:

$$\frac{\partial}{\partial t} j_z(x,t) = \varepsilon_0 \omega_p^2 E_z(x,t), \tag{4}$$

$$\frac{\partial}{\partial t} j_x(x,t) = \varepsilon_0 \omega_p^2 E_x(x,t) + \frac{e}{m_e} j_z(x,t) B_y(x,t) \tag{5}$$

must to be considered (ω_p—plasma frequency). The electric and magnetic fields of standing wave in plasma without collisions and ion current density connected with quiver motion can be described by:

$$E_z(x,t) = 2E_0 \cos(\omega t)\cos(kx), \tag{6}$$

$$B_y(x,t) = -2\frac{E_0}{c_f}\sin(\omega t)\sin(kx), \tag{7}$$

$$j_z(x,t) = 2\frac{\varepsilon_0 \omega_p^2}{\omega} E_0 \sin(\omega t)\cos(kx), \tag{8}$$

where: E_0 is the amplitude of the electromagnetic wave, c_f is the phase velocity. The electrons' movement in the direction of the laser light (x—direction) appears due to the Lorentz force (ponderomotive force): Using (7) and (8) we obtain

$$F_{NL}(x,t) = ev_z(x,t)B_y(x,t) \equiv eE_{NL}(x,t), \tag{9}$$

$$E_{NL}(x,t) = 2E_{NL}\sin^2(\omega t)\sin(2kx),$$

$$E_{NL} = \frac{v_e}{c_f}E_0, v_e = \frac{eE_0}{m_e\omega}. \tag{10}$$

The Lorentz force causes the longitudinal electric field between electron and ion fluid to appear. This field is described by Eqs. (3) and (5). Taking Eqs. (9) and (10) into consideration, the equation for the longitudinal electric field can be obtained:

$$\frac{\partial^2}{\partial t^2} E_x(x,t) + \omega_p^2 E_x(x,t) = 2\omega_p^2 E_{NL}\sin^2(\omega t)\sin(2kx). \tag{11}$$

Using complex notation and assuming that $E_x(x,t)$ has the form:

$$E_{NL}(x,t) \to E_{NL}(x,t) = -2iE_{NL}\sin^2(\omega t)\exp(-2ikx),$$

$$E_x(x,t) = -iE_x(t)\exp(-2ikx) \tag{12}$$

we obtain equation for the amplitude $E_x(t)$:

$$\frac{\partial^2}{\partial t^2} E_x(t) + \omega_p^2 E_x(t) = 2\omega_p^2 E_{NL}\sin^2(\omega t). \tag{13}$$

This pendulum-like equation can be solved analytically. Since ions are too heavy to follow oscillation of the longitudinal electric (oscillation with characteristic frequencies of Eq. (13)—the laser frequency and the plasma frequency), the time average of $E_x(t)$ is important as ions' movement is to be considered. The time average longitudinal electric field does not depend on the initial condition of Eq. (13) and is given by:

$$\langle E_x(x,t)\rangle = \langle E_x(t)\rangle \sin(2kx) = E_{NL}\sin(2kx). \tag{14}$$

The value of the amplitude of the time average longitudinal electric field is given by Eq. (10). Since v_e cannot exceed the velocity of light and phase velocity is higher than the velocity of light, the amplitude of longitudinal electric field is less than the amplitude of the laser field. However, the above expression does not include any relativistic effects and are valid only when v_e is much less than c.

3. MOTION OF IONS—RIPPLING

Bearing in mind the time average longitudinal electric field caused by the motion of electrons, we can consider equations describing the behavior of ions due to this field. Without any simplifications these equations have the form:

https://doi.org/10.1017/S0263034606060046 Published online by Cambridge University Press

$$m_p n_p(x,t)\left(\frac{\partial}{\partial t}v_{px}(x,t)+v_{px}(x,t)\frac{\partial}{\partial x}v_{px}(x,t)\right)$$
$$= en_p(x,t)\langle E_x(x,t)\rangle - \frac{\partial}{\partial x}p_p(x,t), \tag{15}$$

$$\frac{\partial}{\partial t}n_p(x,t) = -\frac{\partial}{\partial x}(n_p(x,t)v_{px}(x,t)), \tag{16}$$

where $\langle E_x(x,t)\rangle$ is given by Eq. (14), v_{ep} is the velocity of proton fluid, m_p and n_p are the proton mass and ion (proton) number density, respectively. During a few moments after the standing wave is switched on (we assume that ion velocity at the beginning is equal to zero and the inhomogeneity of the initial plasma is small), pressure and square term of the Lagrange derivative on the left side of Eq. (15) can be omitted. In this case, we obtain equations describing the rippling of ion density:

$$m_p\frac{\partial}{\partial t}v_{px}(x,t) = eE_{NL}\sin(2kx) \tag{17}$$

$$\frac{\partial}{\partial t}n_p(x,t) = \frac{\partial}{\partial x}(n_p(x,t)v_{px}(x,t)) \approx -n_p(x,t)\frac{\partial}{\partial x}v_{px}(x,t). \tag{18}$$

It is possible to solve the equation of continuity without the simplification made in Eq. (18). However, the omission of square term of Lagrange derivative causes severe restriction. Solution of Eqs. (17) and (18) are given by:

$$v_{px}(x,t) = v_{ep}\frac{v_{ep}}{c_f}(\omega t)\sin(2kx), \tag{19}$$

$$n_p(x,t) = n_i(x)\exp\left\{-\frac{v_{ep}^2}{c_f^2}(\omega t)^2\cos(2kx)\right\}$$
$$\approx n_i(x)\left(1-\frac{v_{ep}^2}{c_f^2}(\omega t)^2\cos(2kx)+\ldots\right), \tag{20}$$

where:

$$v_{ep} \equiv \frac{eE_0}{\sqrt{m_e m_p}\omega}. \tag{21}$$

Let us consider two intensities to show the order of v_{ep}; for $I = 10^{16}$ W/cm^2, v_{ep} is equal to 6.4×10^5 m/s; for $I = 10^{17}$ W/cm^2, v_{ep} is equal 2.0×10^6 m/s. The above expressions describing the rippling are valid when:

$$(\omega t) \ll \frac{c_f}{v_{ep}}. \tag{22}$$

This condition expresses mathematically what has just been described as "a few moments after the standing wave is switched on." Up to this moment, E_0 was the arbitrary amplitude of the electromagnetic wave in plasma. Now let E_0 be the amplitude of a wave in a vacuum. If homogenous plasma is considered, the following transformation in all the above expressions should be done:

$$E_0 \to \frac{2}{1+\eta}E_0, \quad \eta\text{—the refractive index of plasma.} \tag{23}$$

The linearly increasing initial plasma density can also be taken into account. In this case, the "swelling" of the wave electric field should be taken into consideration:

$$E_0 \to \frac{1}{\sqrt{\eta}}E_0. \tag{24}$$

Let us consider the last case. Then expressions describing the rippling take the form ($c_f = c/\eta$):

$$v_{ep}(\eta) = \frac{1}{\sqrt{\eta}}v_{ep} = \frac{1}{\sqrt{\eta}}\frac{eE_0}{\sqrt{m_e m_p}\omega}, \tag{25}$$

$$v_{px}(x,t) = v_{ep}\frac{v_{ep}}{c}(\omega t)\sin(2kx), \tag{26}$$

$$n_p(x,t) = n_i(x)\exp\left\{-\eta\frac{v_{ep}^2}{c^2}(\omega t)^2\cos(2kx)\right\}$$
$$\approx n_i(x)\left(1-\eta\frac{v_{ep}^2}{c^2}(\omega t)^2\cos(2kx)+\ldots\right), \tag{27}$$

$$(\omega t) \ll \frac{1}{\sqrt{\eta}}\frac{c}{v_{ep}}. \tag{28}$$

Figure 1 shows a numerical example of the rippling formation in initially increasing plasma density irradiated by the neodymium laser light. The amplitude of ion density rippling and the velocity of ions do not depend on position which is in agreement with Eqs. (26) and (27). The value of velocity amplitude of ions ($\sim 1.5 \times 10^5$ m/s) is less than v_{ep} for $I = 10^{17}$ W/cm^2 (2.0×10^6 m/s), so condition (28) in the case illustrated in Figure 1 is fulfilled.

3. MOTION OF IONS—THE STATIONARY SOLUTION

Restrictions of (22) or (28) are caused by exclusion of $v_{px}(\partial/\partial x)v_{px}$ term in Eq. (15). Let us try to find the stationary solution of the motion of ions in the longitudinal electric field (9) with this term, but at first neglecting pressure. The following set of equations should be taken into consideration:

https://doi.org/10.1017/S0263034606060046 Published online by Cambridge University Press

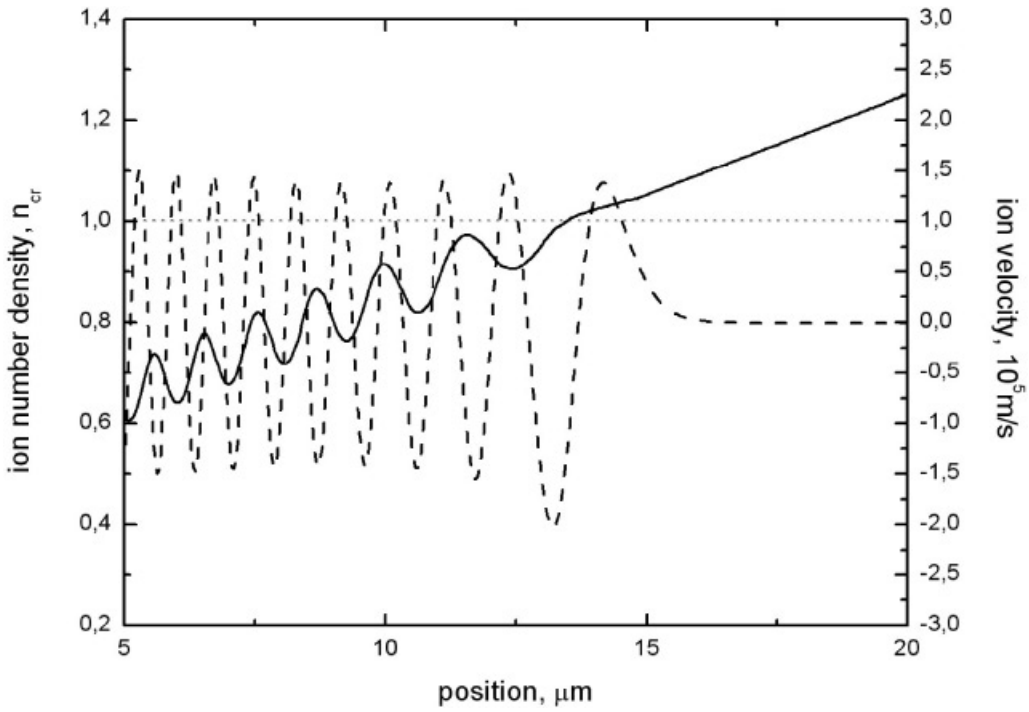

Fig. 1. Numerical example showing formation of rippling in underdense plasma. Density profile (solid line) and velocity of ions (dotted line) are given at time 0.65 ps after laser light ($I = 10^{17}$ W/cm^2, $\tau L = 1$ ps) starts to irradiate hydrogen plasma with linearly increasing density. Initial temperature of protons and electrons is 100 eV.

$$m_p\left(v_{px}(x)\frac{\partial}{\partial x}v_{px}(x)\right) = eE_{NL}\sin(2kx), \tag{29}$$

$$0 = -\frac{\partial}{\partial x}(n_p(x)v_{px}(x)). \tag{30}$$

Eq. (29) is fulfilled by the following function:

$$v_p^{(1)}(x) = \sqrt{2}v_{ep}\sin(kx). \tag{31}$$

Expressions describing the stationary solution of ion motion in plasma without pressure caused by the electromagnetic standing wave are given by:

$$E_z(x,t) = 2E_0\cos(\omega t)\cos(kx), \tag{32a}$$

$$\langle E_x(x,t)\rangle = E_{NL}\sin(2kx), \tag{32b}$$

$$v_p^{(1)}(x) = \sqrt{2}v_{ep}\sin(kx). \tag{32c}$$

The situation described by the above equations is possible when the electromagnetic wave is trapped in plasma between two critical densities (the soliton-like structure). The second critical density is created near the initial critical density by the rippling process described in Section 2. The spatial period of the function (32b) is two times smaller than the spatial period of solution (32c). To give physical meaning to (32a–32c), only one spatial period (32b) should be taken into consideration, for example: $(-\pi/2 < kx < \pi/2)$. In Figure 2 the plot of functions (32a–32c) is shown. This corresponds with the situation when the electromagnetic wave is trapped in plasma deformed by the ion density rippling (E_0 is now the amplitude of trapped electromagnetic field).

At $kx = \pm\,\pi/2$ there is the discontinuity which can be analyzed by taking pressure into account. Non-physicality of the solution of Eq. (29) without pressure is seen also when Eq. (30) is considered: everywhere where ion velocity becomes zero the density goes to infinity. For example, at $kx = 0$ there occurs decompression and ion density should become zero instead of infinity.

Let us consider the equation describing the stationary motion of ions without neglecting pressure:

$$m_p n_p(x)\left(v_{px}(x)\frac{\partial}{\partial x}v_{px}(x)\right) = en_p(x)E_{NL}\sin(2kx) - \frac{\partial}{\partial x}p_p(x), \tag{33}$$

ions' number conservation is described by Eq. (30). Since pressure is taken into consideration, the equation of state of ion fluid should be given. The adiabatic process in an ideal gas is assumed:

$$p_p(x) = n_p(x)k_B T_p(x), \tag{34}$$

$$p_p(x) = const\, n_p^{\gamma}(x), \gamma = \tfrac{5}{3}. \tag{35}$$

https://doi.org/10.1017/S0263034606060046 Published online by Cambridge University Press

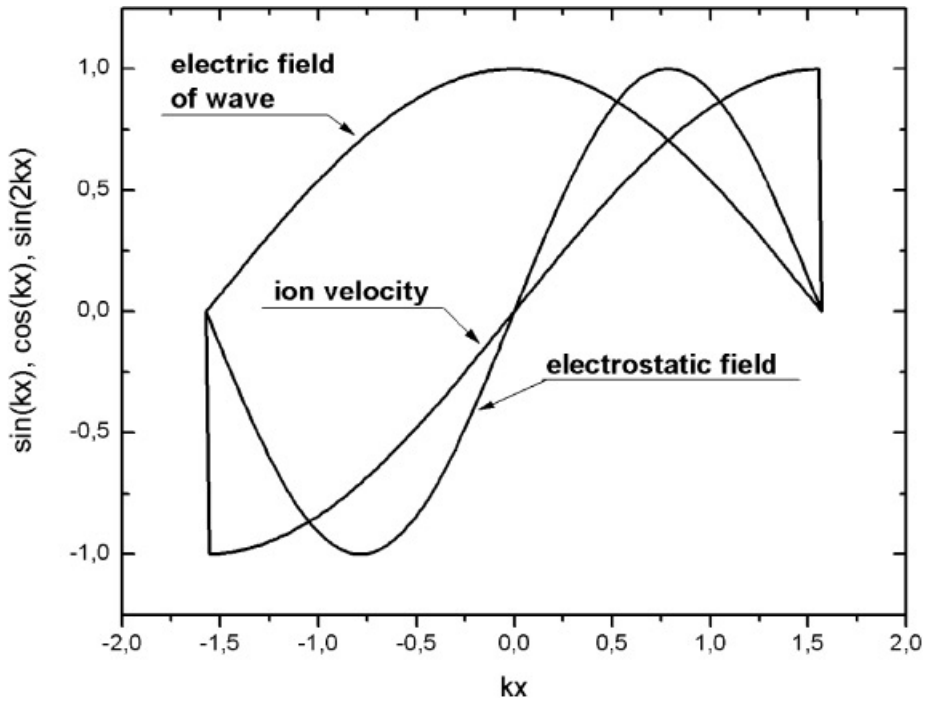

Fig. 2. Functions corresponding with (32a–32c) describing the soliton-like structure in plasma without pressure: i.e., the electric field of the electromagnetic wave trapped in plasma at time $t = 0$, the time average longitudinal electric field and the solution of (29)—ion velocity profile.

Eqs. (30) and (33) were solved under the assumption that the impact of pressure is small everywhere, excluding regions near $kx = 0$ and $kx = \pm \pi/2$. This can be expressed mathematically by the condition $v_{Tp} \ll v_{ep}$ (v_{Tp}—the initial ion thermal velocity). Solution of Eq. (33) is then given by:

$$v_p^{(2)}(x) = \begin{cases} 2v_{Tp} & 0 \le kx \le kx_1 \quad (36) \\ \sqrt{2}v_{ei}\sin(kx) + \dfrac{2v_{Tp}^2}{\sqrt{2}v_{ei}\sin(kx) + v_{Tp}} & kx_1 \le kx < kx_2 \quad (37) \\ 2v_{Tp}\dfrac{\alpha}{\left(\alpha^{1/2} - \dfrac{2\alpha^2}{\pi^2}(1+\cos(2kx))\right)^{3/2}} & kx_2 < kx \le \dfrac{\pi}{2} \quad (38) \end{cases}$$

where:

$$\alpha = \sqrt{\frac{2}{5}}\frac{\pi}{2}\frac{v_{ep}}{v_{Tp}},\ \sin(kx_1) = \sqrt{\frac{1}{5}}\frac{1}{\alpha}\frac{\pi}{2},\ kx_2 = \left(1 - \frac{1}{\alpha^{3/4}}\right)\frac{\pi}{2}. \quad (39)$$

The plot of the above function for laser intensity $I = 10^{17}$ W/cm^2 and for initial ion temperature $T_p = 30$ eV is shown in Figure 3.

Since thermal velocity is small in comparison with v_{Tp}, changes of ion velocity shape are not significant except near $k = 0, \pm \pi/2$. To show the impact of pressure on the shape of ions velocity, numerical calculations were performed in case when 1 ps neodymium laser pulse of intensity $I = 10^{17}$ W/cm^2 irradiates hydrogen plasma of high initial ion temperature $T_p = 1$ keV. Figure 4 shows ion number density and ion velocity profile created 2.2 ps after laser started to interact with plasma.

At $kx = 0$ decompression appears; at $kx = \pi/2$ compression takes place—ion temperature and ion number density increase. Let us consider the last case in a more detailed way. On the basis of the presented model, it can be seen that the compressed plasma moves in two directions: into vacuum (backward direction) and into plasma interior (forward direction) with the thermal velocity of compressed ions. We can calculate the maximum ion number density:

$$(n_p)_S = \alpha^{3/4} n_{cr}, \quad (40)$$

and the maximum temperature of the compressed ions:

$$(k_B T_p)_S = \alpha^{1/2} k_B T_p. \quad (41)$$

Effectiveness of the adiabatic plasma compression is described by the dimensionless coefficient α given by Eq. (39). Let us consider neodymium-glass laser to show the order of α. For the amplitude of the electromagnetic wave in vacuum and

https://doi.org/10.1017/S0263034606060046 Published online by Cambridge University Press

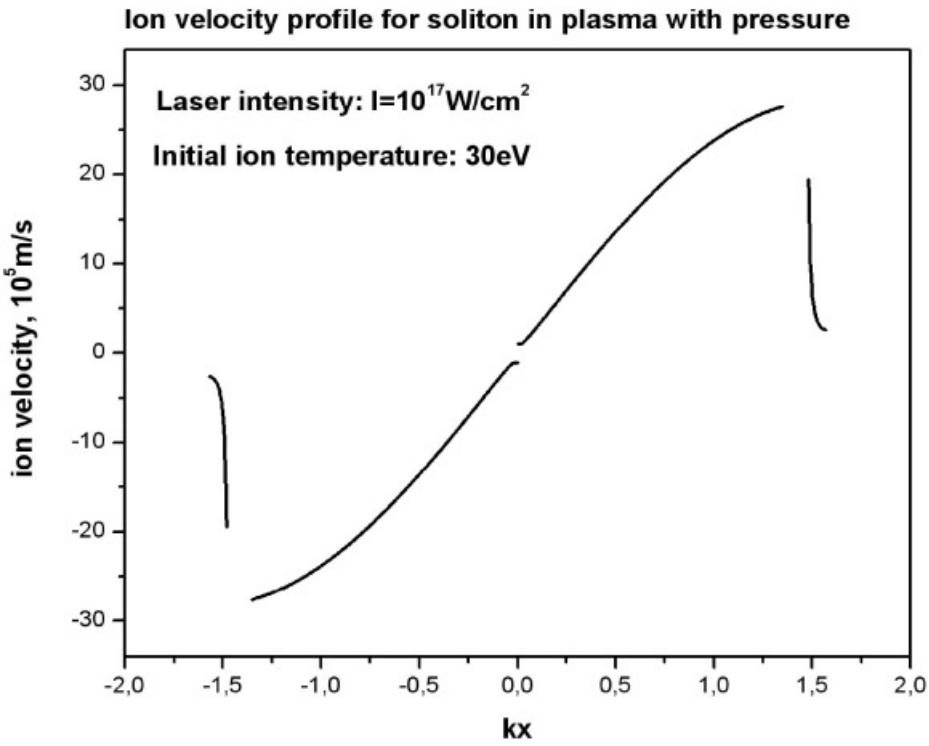

Fig. 3. Plot of function $v(2)\ (x)\ p$ for $I = 10^{17}$ W/cm^2 and for $T = 30$ eV. The values for $kx \in (-\pi/2,0)$ are given from the symmetry of the problem.

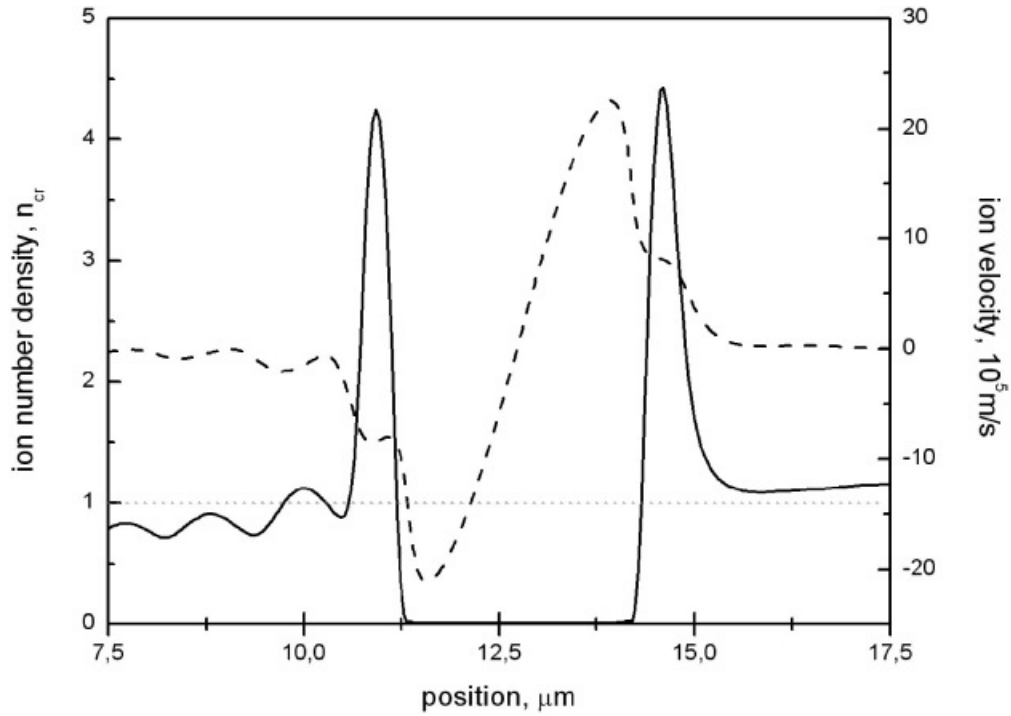

Fig. 4. Ion density (solid line) and ion velocity (dashed line) profile 2.2 ps after neodymium—glass laser ($I = 10^{17}$ W/cm^2) started irradiate hydrogen plasma of the initial temperature $Tp = 1$ keV.

https://doi.org/10.1017/S0263034606060046 Published online by Cambridge University Press

the initial plasma temperature $k_B T_p = 100$ eV we obtain, for example: $\alpha = 6.4$ for $I = 10^{16}$ W/cm^2 ($E_0 = 2.7 \times 10^{11}$ V/m), $\alpha = 20.2$ for $I = 10^{17}$ W/cm^2 ($E_0 = 8.7 \times 10^{11}$V/m).

Pressure consideration also allows calculating the ion current density produced by the soliton–ion number density is given by (40); velocity of ion motion is obtained from formula (38) for $kx = \pi/2$:

$$(j_p)_S = e(n_p)_S(2v_{Tp}a^{1/4}) = 2e(n_p)_S\sqrt{\frac{(k_B T_p)_S}{m_p}}$$

$$= \sqrt{\frac{2}{5}}\pi(ev_{ep}n_{cr}). \quad (42)$$

From Eqs. (40 to 42) it is seen that the motion of ions caused by the trapped electromagnetic wave is characterized by the initial ion temperature and the value of the amplitude of the soliton electric field (E_0). This amplitude—as numerical calculations show—is usually less than the amplitude of the electric field of light a wave in vacuum. Additionally, it decreases because of the energy transmission from the soliton to ions and because of the plasma trap expansion (ions move in the opposite direction). However, the changes of the electric field are small and the assumption that E_0 does not vary during and after the steady state creation is valid.

Let us consider a case when 1 ps neodymium glass laser pulse of intensity $I = 10^{17}$ W/cm^2 interacts with hydrogen plasma of initial temperature $T = 100$ eV. Figure 5 illustrates the ion number density profile and the electric field trapped between two critical densities at 1.7 ps. The amplitude of the electric field of the soliton-like structure is in this case equal to about 5×10^{11} V/m. For this value, from Eqs. (39 to 42) we obtain: $\alpha = 11.7$, $\sqrt{2}v_{ep} = 1.6 \times 10^6$ m/s, $(n_p)_S = 6.3\, n_{cr}$, $(k_B T_p)_S = 342$ eV, $(j_p)_S = 3.8 \times 10^{10}$ A/cm^2. Figure 6 shows the ion velocity profile and the ion number density at 2.4 ps. In this case: the maximum ion current density is equal to $\sim 4.4 \times 10^{10}$ A/cm^2; the amplitude of stationary ions motion is equal $\sim 1.5 \times 10^6$ m/s, which is in good agreement with values obtained from analytical calculations. However, the ion number density obtained by numerical calculation is less than these one obtained analytically. It can be explained by a very high ion density gradient which takes place in this process and numerical problems to maintain such a gradient.

4. BROAD BAND PICOSECOND LASER SMOOTHING

The ion density rippling process described in Section 2 results in the increase of reflection from plasma before mirror reflection from the critical density (Boreham *et al.*, 1997; Jablonski *et al.*, 2005). This causes only a small part of the laser pulse to be trapped near the critical density. Rippling can be attenuated when the laser pulse consists of not only one frequency component. Let the electric field of wave be built of m components with different frequencies:

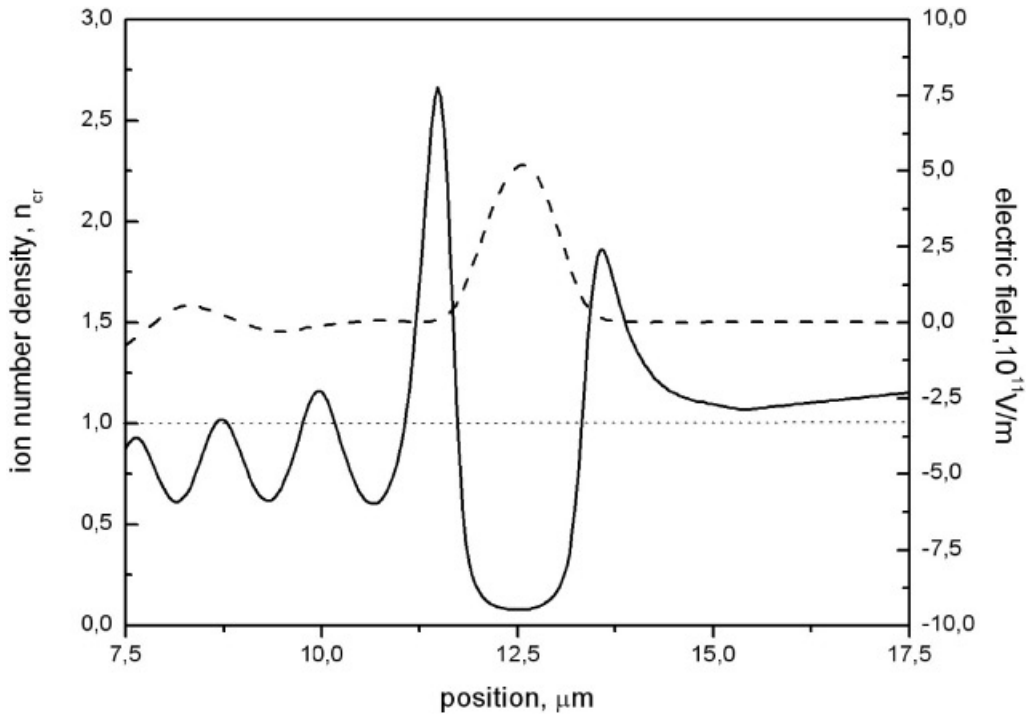

Fig. 5. Ion density (straight line) and trapped electric field (dashed line) 1.7 ps after neodymium glass laser $I = 10^{17}$ W/cm^2 started to irradiate hydrogen plasma of initial temperature $Tp = 100$ eV. The amplitude of trapped electromagnetic field ($\sim 5 \times 10^{11}$ V/m) is not much less than the one of wave in vacuum (8.7×10^{11} V/m).

https://doi.org/10.1017/S0263034606060046 Published online by Cambridge University Press

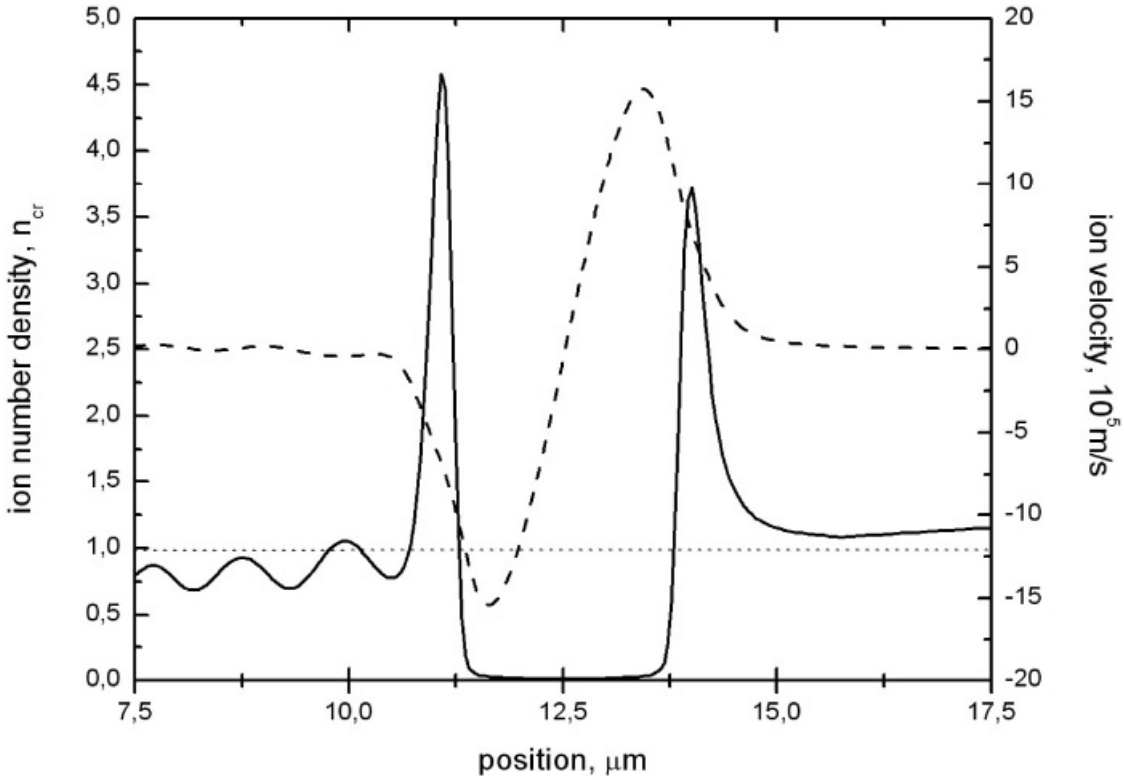

Fig. 6. Ion density (straight line) and ion velocity profile (dashed line) at 2.4 ps after neodymium glass laser $I = 10^{17}$ W/cm^2 started irradiate deuterium plasma of initial temperature $T = 100$ eV.

$$E_z(x,t) = \sum_{n=1}^{m} \frac{E_0}{m} \cos(\omega_n t - k_n x), \tag{43}$$

where:

$$\{\omega_n\} = \omega_0 \pm \Delta\omega, \omega_0 \pm 2\Delta\omega, \ldots, \omega_0 \pm \frac{m}{2}\Delta\omega \quad \text{for } m\text{—even;}$$

$$\{\omega_n\} = \omega_0, \omega_0 \pm \Delta\omega, \ldots, \omega_0 \pm \frac{m-1}{2}\Delta\omega \quad \text{for } m\text{—odd.}$$

For the laser pulse constructed in this way, the time average longitudinal electric field equals:

$$\langle E_x(x,t)\rangle = \frac{1}{m} E_{NL} \sin(2k_0 x). \tag{44}$$

Eq. (44) is valid when the following conditions are satisfied:

$$\Delta\omega \ll \omega_0, \frac{\Delta\omega > \pi}{\tau'} \quad (\tau\text{—laser pulse duration}). \tag{45}$$

The first condition of (45) allows assuming that the wave numbers k_n ($n = 1, 2, \ldots m$) can be approximated by k_0. It also has an effect upon the critical density for each component of (43), as it does not differ much from the critical density for ω_0. In order to use the time average of the electric field for different components, the second condition is necessary. For the time average longitudinal electric field given by (44), expressions describing rippling have the form:

$$v_{px}^{(m)}(x,t) = \frac{1}{m}\frac{v_{ep}^2}{c}(\omega t)\sin(2kx), \tag{46}$$

$$n_p^{(m)}(x,t) \approx n_i(x)\left(1 - \frac{\eta}{m}\frac{v_{ep}^2}{c^2}(\omega t)^2\cos(2kx) + \ldots\right). \tag{47}$$

From (47) it can be seen that, in comparison with (26, 27), ion density rippling decreases like 1/m. Figure 7 shows the result of the numerical calculation performed for the laser light combined with three waves ($\Delta\omega_0 = 0.5\%\ \omega_0$). The ion number density shape and the ion velocity profile 0.8 ps after electromagnetic field started to interact with plasma is presented. In comparison with Figure 1, which shows the result of the interaction of one frequency component laser light, it is seen that even though the time of the interaction is longer, the ion density rippling is smaller.

Since the time average longitudinal electric field is also responsible for the processes described in Sections 3 and 4, it is possible to obtain the expressions for the soliton-like

https://doi.org/10.1017/S0263034606060046 Published online by Cambridge University Press

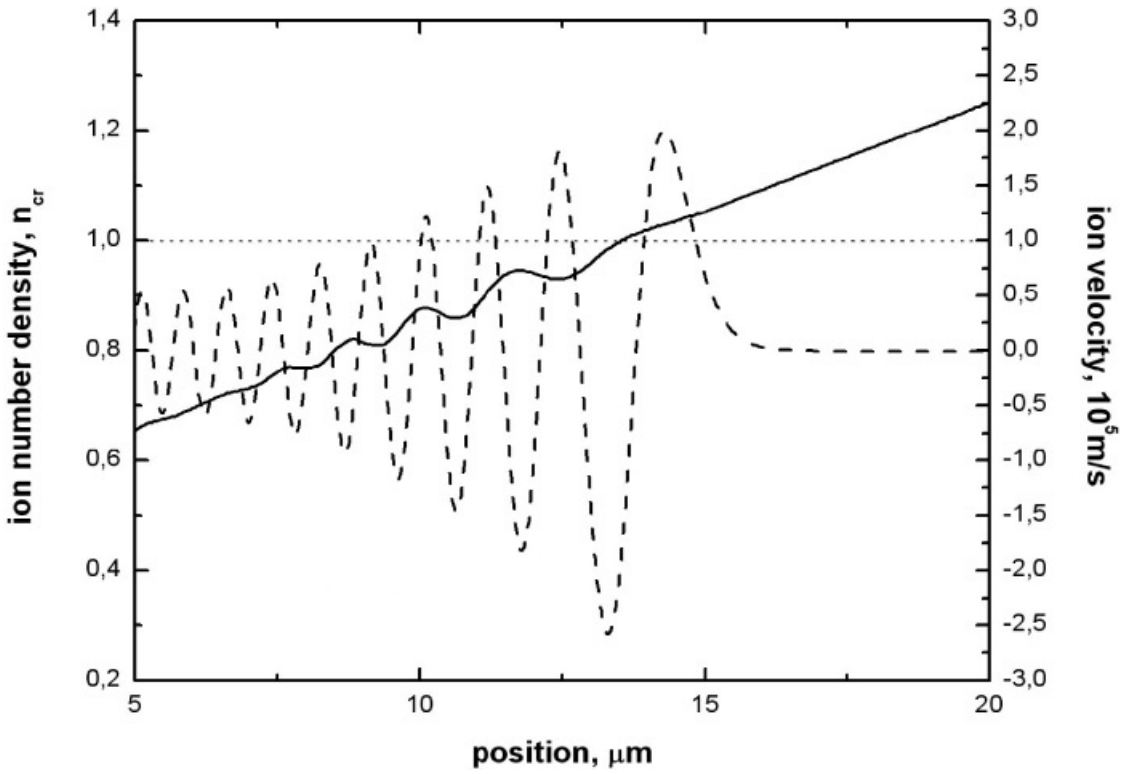

Fig. 7. Ion density (solid line) and ion velocity profile (dashed line) 0.8 ps after the laser pulse consisted with tree frequencies components (ω—neodymium laser, $\Delta\omega = 0.5\%\ \omega 0$) started to irradiate hydrogen plasma of initial temperature and initial ion density profile as in Figure 1.

structure created by the laser pulse consisting of different frequencies (43). In this case, the values corresponding with v_{ep} and with the coefficient α are given by:

$$v_{ep}^{(m)} = \frac{1}{\sqrt{m}} \frac{eE_0}{\sqrt{m_e m_p}\omega}, \tag{48}$$

$$\alpha^{(m)} = \sqrt{\frac{2}{5}} \frac{\pi}{2} \frac{v_{ep}^{(m)}}{v_{Tp}} = \frac{1}{\sqrt{m}} \sqrt{\frac{2}{5}} \frac{\pi}{2} \frac{v_{ep}}{v_{Tp}}. \tag{49}$$

It is seen that the velocity (48) and the coefficient $\alpha^{(m)}$ describing the ion compression decrease like the square root of m—slower than the ion density rippling (47).

Basing on (48) and (49) it is possible to calculate (compare with (40–42)):

1. the maximum ion density:

$$(n_p^{(m)})_S = (\alpha^{(m)})^{3/4} n_{cr} = \frac{1}{m^{3/8}} \alpha^{3/4} n_{cr} \tag{50}$$

2. the maximum ion temperature:

$$(k_B T_p^{(m)})_S = (\alpha^{(m)})^{1/2} k_B T_p = \frac{1}{m^{1/4}} \alpha^{1/2} k_B T_p \tag{51}$$

3. the maximum ion current density:

$$(j_p^{(m)})_S = 2e(n_p^{(m)})_S \sqrt{\frac{(k_B T_p^{(m)})_S}{m_p}} = \frac{1}{\sqrt{m}} \sqrt{\frac{2}{5}} \pi (e v_{ep} n_{cr}). \tag{52}$$

The effectiveness of the decrease in ion density rippling can be expressed not only by reflectivity changes but also by the value of the electric field amplitude of the soliton-like structure. Figure 8 shows the ion density and the ion velocity profile created by the electromagnetic field at time 1.5 ps. In this case, electric field amplitude of soliton was about 1.5×10^{12} V/m. The time necessary for the creation of the steady-state is smaller than in the case when laser pulse consists of only with one frequency component—it is also the effect of decreasing rippling. Using Eqs. (49–52) for $E_0 = 1.5 \times 10^{12}$ V/m and for the initial ion temperature $T_p =$ 100 eV we obtain:

$$\alpha^{(3)} = 20.2,\ \sqrt{2} v_{ep}^{(3)} = 2.8 \times 10^6 \text{ m/s},\ (n_p^{(3)})_S = 9.5\ n_{cr},$$

$$(k_B T_p^{(3)})_S = 450 \text{ eV},\ (j_p^{(3)})_S = 6.3 \times 10^{10} \text{ A/cm}^2.$$

The ion amplitude velocity of stationary motion obtained by numerical calculation is about 2.5×10^6 m/s; maximum ion

https://doi.org/10.1017/S0263034606060046 Published online by Cambridge University Press

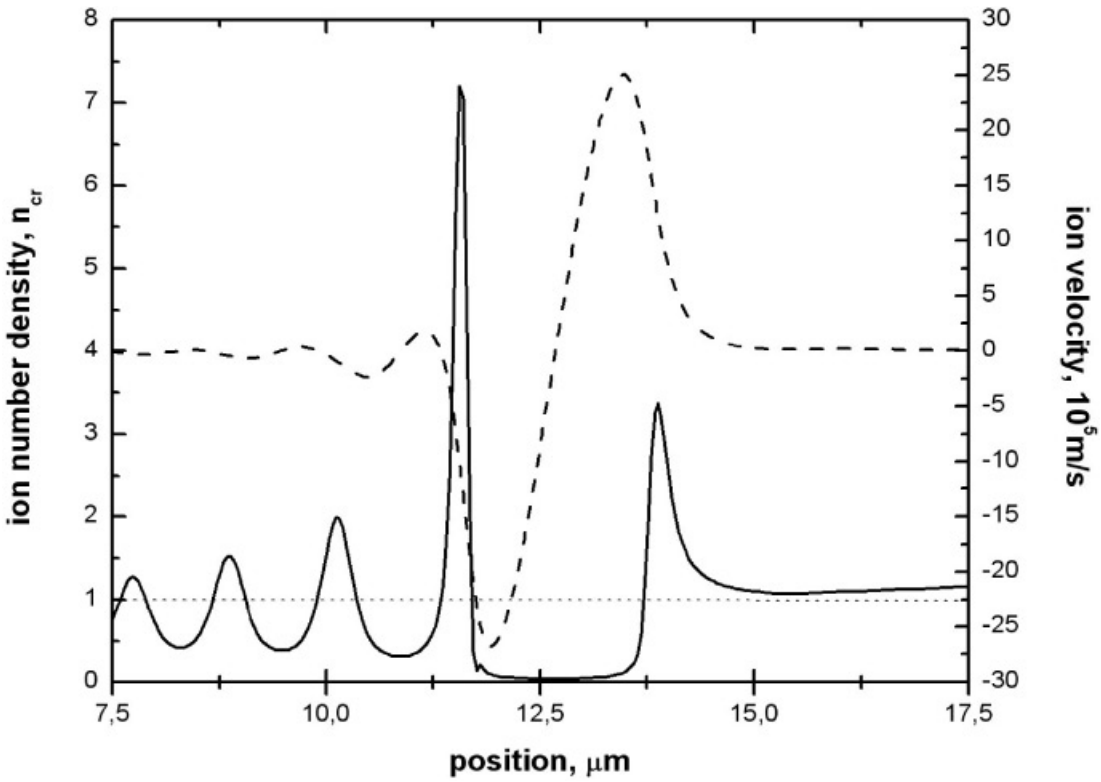

Fig. 8. Ion density (solid line) and ion velocity profile (dashed line) at 1.5 ps after laser pulse consists of tree frequencies ($\omega 0$—neodymium laser, $\Delta\omega = 0.5\%\ \omega 0$) started to irradiate hydrogen plasma of initial temperature $Tp = 100$ eV and initially linearly increasing ion density profile.

current density obtained in this case equals about 7.8×10^{10} A/cm^2 which is in good agreement with analytical calculations.

5. CONCLUSION

It has been shown that the electromagnetic field trapped in plasma near the critical density surface can result in generation of high-current-density ion beams propagating in two opposite directions. It is possible that this phenomenon is responsible for the observed features of the ion beams measured in the experiments in which the subrelativistic, picosecond laser pulses interact with the preplasma created in the front of the solid target. More detailed numerical calculations for different properties of the initial plasma ramp (initial gradient density, initial temperature, and chemical composition of plasma) and for different laser pulse characteristics (pulse duration, intensity, and shape) should be performed to probe this possibility. Such calculations will also allow better comparison with experimental results and better understanding their physical background. Since the relativistic, subpicosecond laser pulses are technically obtainable, it would be worth investigating the impact of the relativistic phenomena on ion density rippling and on the properties of soliton-like structures produced near the critical surface.

ACKNOWLEDGMENTS

This work was supported in part by the State Committee for Scientific Research (KBN), Poland under Grant No 1 PO3B 043 26 and by a grant for a Visiting Scientist by the University of Western Sydney, Australia. .

REFERENCES

Asthana, M.V., Giulietti, A., Giulietti, L.A. & Sodha, M.S. (2000). Relativistic interaction of rippled laser beams with plasmas. *Laser Part. Beams* **18**, 399–403.

Badziak, J., Glovacz, S.G., Jablonski, S., Parya, P., Wolowsk, J. & Hora, H. (2004*a*). Production of ultrahigh-current-density ion beams by short-pulse skin-layer laser-plasma interaction. *Appl. Phys. Lett.* **85**, 3042–3047.

Badziak, J., Glowacz, S., Jablonski, S., Paris, P., Wolowski J., Kraska, J., Laska L., Rohlena, K. & Hora, H. (2004*b*). Production of ultrahigh ion current densities at Akin-Layer subrelativistic laser-plasma interaction. *Plasma Phys. Contr. Fusion* **46**, B541–B555.

Badziak, J., Glowacz, S., Jablonski, S., Parys., P., Wolowski, J. & Hora, H. (2005). Laser driven generation of high-current ion beams using skin-layer ponderomotive acceleration. *Laser Part. Beams* **23**, 401–409.

Bauer, D. (2003). Plasma formation through field ionization intense laser-matter interaction. *Laser Part. Beams* **21**, 489–495.

https://doi.org/10.1017/S0263034606060046 Published online by Cambridge University Press

Boreham, B.W., Hora, H., Aydin, M., Eliezer, S., Goldsworthy, M.P., Gu Min, Ghatiak, A.K., Lalousis, P., Stening, R.J., Szichman, H., Luther-Davies, B., Baldwin, K.G.H., Maddever, R.A.M. & Rode, A.V. (1997). Beam smoothing and temporal effects: Optimized preparation of laser beam for direct drive inertial confinement fusion. *Laser Part. Beams* **15**, 277–295.

Cang, Y., Osman, F., Hora, H., Zhang, J., Badziak, J., Wolowski, J., Jungwirth, K., Rohlena, K. & Ullschmied, J. (2005). Computations for nonlinear force driven plasma blocks by picosecond laser pulses for fusion. *J. Plasma Phys.* **71**, 35–51.

Deutsch, C. (2004). Penetration of intense charge particle beams in the outer layers of precompressed thermonuclear fuels. *Laser Part. Beams* **22**, 115–120.

Glowacz, S., Badziak, J., Jablonski, S. & Hora, H. (2004). Numerical investigation of generation of high-current ion beams by short-pulse laser plasma interaction. *Czech. J. Phys.* **54**, C460.

Hoffmann, D.H.H., Blazevic, A., Ni, P., Rosmej, O., Roth, M., Tahir, N.A., Tauschwitz, A., Udrea, S., Varentsov, D., Weyrich, K. & Maron, Y. (2005). Present and future perspectives for high energy density physics with intense heavy ion and laser beams. *Laser Part. Beams* **23**, 47–53.

Hoffmann, D.H.H., Weyrich, K., Wahl, H., Gardes, D., Bimbot, R. & Fleurier, C. (1990). Energy-loss of heavy-ions in a plasma target. *Phys. Rev. A* **42**, 2313–2321.

Hora, H. & Aydin, M. (1992). Suppression of stochastic pulsation in laser-plasma interaction by smoothing methods. *Phys. Rev. A* **45**, 6123–6126.

Hora, H. & Aydin, M. (1999). Increased gain for ICF with red light at suppression of stochastic pulsation by smoothing. *Laser Part. Beams* **17**, 209–215.

Hora, H. (1991). *Plasmas at High Temperature and Density*. Heidelberg: Springer.

Hora, H. (2004). Developments in inertial fusion energy and beam fusion at magnetic confinement, *Laser Part. Beams* **22**, 439–449.

Hora, H., Badziak, J., Boody, F., Höpfl, R., Jungwirth, K., Kralikowa, B., Kraska, J., Laska, L., Parys, P., Perina, V., Pfeifer, K. & Rohlena, J. (2002). Effects of ps and ns. laser pulses for giant ion source. *Optics Commun.* **207**, 333–338.

Jablonski, S., Hora, H., Glowacz, S., Badziak, J., Cang Yu. & Osman, F. (2005). Two-fluid computation of plasma block dynamics for numerical analyze of rippling effect. *Laser Part. Beams* **23**, 433–440.

Mulser, P. & Bauer, D. (2004). Fast ignition of fusion pellets with superintense lasers: Concepts, problems, and prospectives. *Laser Part. Beams* **22**, 5–12.

Mulser, P. & Schneider, R. (2004). On the inefficiency of hole boring in fast ignition. *Laser Part. Beams* **22**, 157–162.

Osman, F., Cang, Y., Hora, H., Cao, L.H., Liu, H., Badziak, J., Parys, A.B., Wolowski, J., Worya, E., Jungwirth, K., Kralikova, B., Kraska, J., Laska, M., Pfeifer, M., Rohlena, K., Skala, J. & Ullschmied, J. (2004). Skin depth plasma front interaction mechanism with prepulse suppression to avoid relativistic self-focusing for high-gain laser fusion. *Laser Part. Beams* **22**, 83–87.

Purohit, G., Pandey, H.D. & Sharma, R.P. (2003). Effect of cross focusing of two laser beams on the growth of laser ripple in plasma. *Laser Part. Beams* **21**, 567–572.

Ramirez, J., Ramis, R. & Sanz, J. (2004). One-dimensional model for a laser-ablated slab under acceleration. *Laser Part. Beams* **22**, 183–188.

Saini, M.S. & Gill, T.S. (2004). Enhanced raman scattering of a rippled laser beam in magnetized collisional plasma. *Laser Part. Beams* **22**, 35–40.